JOURNAL OF VIROLOGY, Nov. 2009, p. 11064–11077 Vol. 83, No. 21
0022-538X/09/$12.00 doi:10.1128/JVI.01016-09

Dynamin- and Lipid Raft-Dependent Entry of Decay-Accelerating Factor (DAF)-Binding and Non-DAF-Binding Coxsackieviruses into Nonpolarized Cells[▽]

Kunal P. Patel,[1,2] Carolyn B. Coyne,[3] and Jeffrey M. Bergelson[1,2]*

Division of Infectious Diseases, Children's Hospital of Philadelphia, Philadelphia, Pennsylvania 19104[1]; University of Pennsylvania School of Medicine, Philadelphia, Pennsylvania 19104[2]; and Department of Cell Biology and Physiology, University of Pittsburgh, Pittsburgh, Pennsylvania 15261[3]

Received 19 May 2009/Accepted 18 August 2009

Group B coxsackieviruses (CVB) use the CVB and adenovirus receptor (CAR) to enter and infect cells. Some CVB also bind to decay-accelerating factor (DAF), but that interaction alone is insufficient for infection. We previously found that CVB3 entry into polarized human intestinal cells (Caco-2) occurs by a caveolin-dependent but dynamin-independent mechanism that requires DAF-mediated tyrosine kinase signals. In this study, we examined how CVB enter and infect nonpolarized HeLa cells and how DAF binding affects these processes. Using immunofluorescence microscopy and a combination of dominant-negative proteins, small interfering RNAs, and drugs targeting specific endocytic pathways, we found that both DAF-binding and non-DAF-binding virus isolates require dynamin and lipid rafts to enter and infect cells. Unlike what we observed in Caco-2 cells, CVB3 entered HeLa cells with CAR. We found no role for clathrin, endosomal acidification, or caveolin. Inhibition of tyrosine kinases blocked an early event in infection but did not prevent entry of virus into the cell. These results indicate that CVB3 entry into nonpolarized HeLa cells differs significantly from entry into polarized Caco-2 cells and is not influenced by virus binding to DAF.

Cells use multiple endocytic pathways to internalize soluble factors and recycle surface proteins. Although some bacteriophages are known to inject their nucleic acid directly into the host cell, most animal viruses rely on endocytic pathways to enter cells and deliver their genomes (34). Two of the best-studied endocytic pathways are mediated by clathrin or caveolin. In clathrin-mediated endocytosis, clathrin and multiple adaptor molecules coat vesicles and induce their internalization (65, 73). Caveolin associates with cholesterol-rich lipid raft domains to promote the formation of caveolar vesicles (44, 51). Both clathrin-mediated and caveolar endocytosis typically require the function of dynamin 2, a GTPase that aids in the fission of endocytic vesicles from the plasma membrane (18, 42, 67). A number of other dynamin-dependent and dynamin-independent endocytic pathways—some involving lipid rafts, but not caveolin—have been described but are less well characterized (reviewed in references 20 and 34).

Group B coxsackieviruses (CVB) are nonenveloped, single-stranded, positive-sense RNA viruses that belong to the enterovirus genus within the *Picornaviridae* family. They are human pathogens that cause febrile illnesses, meningitis, and myocarditis (22, 50). There are six CVB serotypes (CVB1 to -6), all of which bind to the coxsackievirus and adenovirus receptor (CAR) (4, 5, 35). CAR induces conformational changes in the virus capsid that are thought to be essential for release of the RNA genome (39), and the interaction between CVB and CAR on transfected rodent cells is required and sufficient for infection (4). Some CVB isolates also bind to decay-accelerating factor (DAF); however, DAF does not induce conformational changes in the capsid, and virus interaction with DAF is not sufficient for infection (6, 39, 55). Nonetheless, many CVB isolates and many other enteroviruses bind to DAF, suggesting it may play an important role in virus pathogenesis (3).

In polarized epithelial cells, DAF is required for infection because CAR is sequestered in intracellular tight junctions and inaccessible to virus at the apical cell surface. Recent work with Caco-2 cells (15, 17), a polarized intestinal epithelial cell line, demonstrated that the RD strain of CVB3 binds to DAF on the apical surface and is then transported to the tight junction, where it interacts with CAR. By binding to DAF, virus initiates specific kinase signals that are required both for translocation to the tight junction and for subsequent internalization. Virus entry into Caco-2 cells depends on caveolin but not dynamin or clathrin and shows some features typically associated with macropinocytosis. CAR is not internalized with virus (15, 17).

In polarized cells, such as Caco-2, the sorting of DAF and CAR to different membrane domains presents a unique obstacle to virus entry. In nonpolarized cells, such as HeLa cells, both CAR and DAF are accessible on the cell surface and both DAF-binding and non-DAF-binding virus isolates infect efficiently. It is unknown if the virus entry pathway in HeLa and other nonpolarized cells is the same as that used to enter polarized Caco-2 cells. It is also unknown whether in HeLa cells the capacity of virus to bind to secondary receptors, such as DAF, affects the virus entry mechanism. DAF-mediated signals, which are required for entry of virus in Caco-2 cells, could influence how virus enters and infects. Also, the association of DAF with specific membrane compartments or with

* Corresponding author. Mailing address: Children's Hospital of Philadelphia, 3615 Civic Center Blvd., Division of Infectious Diseases, Abramson Research Building Room 1202, Philadelphia, PA 19104. Phone: (215) 590-3771. Fax: (215) 590-2025. E-mail: bergelson@email.chop.edu.

▽ Published ahead of print on 26 August 2009.

specific endocytic pathways could influence how virus enters. DAF-binding and non-DAF-binding isolates of echovirus 11, a closely related enterovirus, have different sensitivities to cholesterol depletion and cytoskeleton disruption, suggesting potential differences in their entry pathways (60). For vaccinia virus, the capacity to bind to glycosoaminoglycans has been reported to correlate with the use of pH-dependent versus pH-independent entry pathways (2).

Other investigators have provided evidence that in HeLa cells CVB3 infection involves dynamin (13, 33), as well as clathrin and endosomal acidification (13). However, the reagents used to demonstrate the roles of clathrin and acidification were not highly specific, endocytic inhibitors were not shown specifically to affect virus entry rather than infection, and it was not made clear whether the CVB3 isolate studied did or did not bind to DAF.

In this work, we have examined the cellular factors required for entry and infection of HeLa CCL-2 cells by CVB3-Nancy, a prototype CVB isolate that does not bind to DAF, and by CVB3-RD, a DAF-binding derivative of Nancy that was used to examine entry in polarized Caco-2 cells (15, 17, 49). We used inhibitors targeting specific endocytic pathways to determine the importance of those pathways for virus infection. Where inhibition of a pathway blocked infection, we tested whether the same inhibitors blocked entry (defined in this study as uptake of viral particles) to verify that these endocytic pathways were required for entry rather than for a postentry event in infection.

We find that entry and infection by CVB3-RD into HeLa CCL-2 cells requires dynamin and lipid rafts but not clathrin, caveolin, or endosomal acidification. This entry mechanism differs significantly from the entry pathway for CVB3-RD in Caco-2 cells. The same inhibitors that block CVB3-RD infection also block infection by CVB3-Nancy, suggesting, to our surprise, that DAF-binding capacity has no effect on the viral entry mechanism. We find a role for tyrosine kinases early in infection; however, they do not appear to be necessary for entry of virus particles.

MATERIALS AND METHODS

Cells and viruses. All experiments were performed on low-passage HeLa cells acquired from the ATCC (HeLa CCL-2 cells). HeLa CCL-2 cells were maintained in minimal essential medium supplemented with 10% fetal bovine serum (FBS) and 1% penicillin-streptomycin, nonessential amino acids, and sodium pyruvate (Invitrogen, Carlsbad, CA). Chinese hamster ovary (CHO) cells stably transfected with cDNA constructs encoding human CAR (CHO-CAR), human DAF (CHO-DAF), or vector alone (CHO-pcDNA) have been previously described (56, 69).

CVB3-RD and CVB3-Nancy were originally obtained from Richard Crowell (Hahnemann University) and expanded as previously described (6, 49). Because CVB3 formed poor plaques in HeLa CCL-2 cells, titers were determined by plaque assay on another laboratory HeLa cell line. Vesicular stomatitis virus (VSV) was provided by Ron Harty (University of Pennsylvania) and was expanded in and titers determined by plaque assays on BHK-21 cells (25).

Antibodies. For immunofluorescence, mouse anti-enterovirus VP1 monoclonal antibody (NCL-Entero; clone 5-D8/1 [71, 72]) was obtained from Leica, and affinity-purified rabbit anti-CAR has previously been described (56). We used goat secondary antibodies conjugated to fluorescein isothiocyanate (FITC) (Jackson Immunoresearch, West Grove, PA) or Alexa Fluor 405 or 547 (Invitrogen, Carlsbad, CA).

For immunoblots, rabbit anti-dynamin 2 (catalog no. ab3457) from Abcam (Cambridge, MA), mouse anti-clathrin heavy chain (catalog no. 610499) and rabbit anticaveolin (catalog no. 610060) from BD Transduction (San Jose, CA), and rabbit anti-glyceraldehyde-3-phosphate dehydrogenase (GAPDH)-horseradish peroxidase (catalog no. sc-25778) from Santa Cruz Biotechnology (Santa Cruz, CA) were used. Secondary antibodies conjugated to horseradish peroxidase were purchased from Santa Cruz.

Plasmids, small interfering RNAs (siRNAs), and pharmacological inhibitors. Green fluorescent protein (GFP)-tagged wild-type (WT) and K44A dominant-negative (DN) dynamin 2 were provided by Mark McNiven (Mayo Institute, Rochester, MN) (10). WT caveolin-1 (Cav-1)-GFP and DN GFP–Cav-1 were provided by Ari Helenius and Lucas Pelkmans (Swiss Federal Institute of Technology, Zurich) (47). Cells (1×10^6 cells/transfection) were transfected with 10 μg of plasmids using the Nucleofector system (Amaxa, Gaithersburg, MD) according to the manufacturer's protocol. Cells were plated at 2.5×10^5 cells per well on chamber slides and infected 36 h later. Transfection efficiencies (determined by GFP expression) ranged between 65 and 80%.

Pooled validated siRNAs targeting dynamin 2 (catalog no. M-004007-03), clathrin heavy chain (catalog no. M-004001-00), Cav-1 (catalog no. M-003467-01), and Cav-2 (catalog no. M-010958-00) were purchased from Dharmacon (Chicago, IL). Negative control siRNA (catalog no. AM4635) was purchased from Ambion (Austin, TX). Cells were serially transfected with siRNAs using Lipofectamine 2000 (Invitrogen, Carlsbad, CA). Briefly, cells were plated in six-well plates at 40% confluence (4×10^4 cells) in antibiotic-free medium and transfected with 167 pmol siRNA the next day (day 1). Cells were washed the following morning (day 2) and replated on day 3. A second transfection was performed on day 4. Cells were replated in chamber slides or 24-well plates for blots on day 5, and experiments were performed the next day. Protein depletion was determined by immunoblotting. For experiments targeting both Cav-1 and Cav-2 together, 167 pmol of each siRNA was used.

Dynasore, genistein, PP2, and bafilomycin A1 were obtained from Calbiochem (La Jolla, CA); chlorpromazine (CPZ), filipin III, NH_4Cl, methyl-beta-cyclodextrin (MβCD), and water-soluble cholesterol from Sigma (St. Louis, MO); and imatinib from LC Laboratories (Woburn, MA). CPZ, NH_4Cl, imatinib, MβCD, and water-soluble cholesterol stock solutions were made in sterile water; stock solutions of the other inhibitors were made in dimethylsulfoxide (DMSO). For drug experiments, cells were pretreated for 45 to 60 min and drug was present during virus binding. Drugs were present for the first 3 h of infection with the exception of the CPZ, NH_4Cl, bafilomycin A1, and imatinib experiments, in which the drug was present for the total time of infection. In some experiments, cells were not pretreated and drugs were added only at the noted time after the start of infection and remained until the end of infection. For experiments with MβCD, a fast-acting drug that extracts cholesterol from the plasma membrane, cells were pretreated with MβCD for 45 min and drug was not used again during the course of infection. In experiments with MβCD where cholesterol was added back, MβCD-treated cells were exposed to 0.25 mM water-soluble cholesterol with 1.4 mM MβCD (to help keep cholesterol in solution). Complete medium with 10% NuSerum (BD Biosciences, Bedford, MA) in place of FBS was used for lipid raft disruption and dynasore experiments since serum components can decrease the efficacy of those drugs (28).

Virus infection and entry assays. For both infection and virus particle uptake experiments, cells were plated on eight-well chamber slides coated with poly-D-lysine (BD Biosciences, San Jose, CA) at $(1.5 \text{ to } 2.0) \times 10^5$ cells/well (for infection experiments) or at 7.5×10^4 cells/well (for particle entry experiments). Virus in binding buffer (minimal essential medium with 20 mM HEPES) was allowed to bind to cells for 1 h at 16°C at 5 PFU/cell (CVB3-RD) or 30 PFU/cell (CVB3-Nancy) for infection experiments and 250 PFU/cell (CVB3-RD) for entry experiments. A higher multiplicity of infection was used for CVB3-Nancy in order to achieve a level of infection (~15 to 20% of cells) similar to that with CVB3-RD. The relatively high multiplicities of infection required might reflect the fact that titers were obtained with a different HeLa cell line than the HeLa CCL-2 cell line from the ATCC that was used for experiments.

Unbound virus was washed off, complete medium was added, and cells were placed at 37°C to initiate infection or virus particle entry. Infection experiments were ended at 6 h with fixation and permeabilization with a 3:1 mixture of ice-cold methanol:acetone for 2 min at room temperature. Virus particle entry was stopped by fixation with 4% paraformaldehyde (PFA) for 15 min at room temperature. Excess PFA was removed with PBS washes and a 5-min treatment with PBS–50 mM NH_4Cl.

For measurements of infection, cells were stained with antiviral antibody as described below ("Immunofluorescence microscopy" section). Three to four fields at 10× objective were captured per well (total of 2,000 to 3,000 cells per well). Each well was treated as a separate sample for analysis. The percentage of cells expressing newly synthesized viral antigen was determined. Results obtained for inhibitor-treated cells were normalized to results obtained for control cells. Quantification of infection was performed using the ImageJ (National Institutes of Health) and Adobe Photoshop (Adobe Systems) software programs.

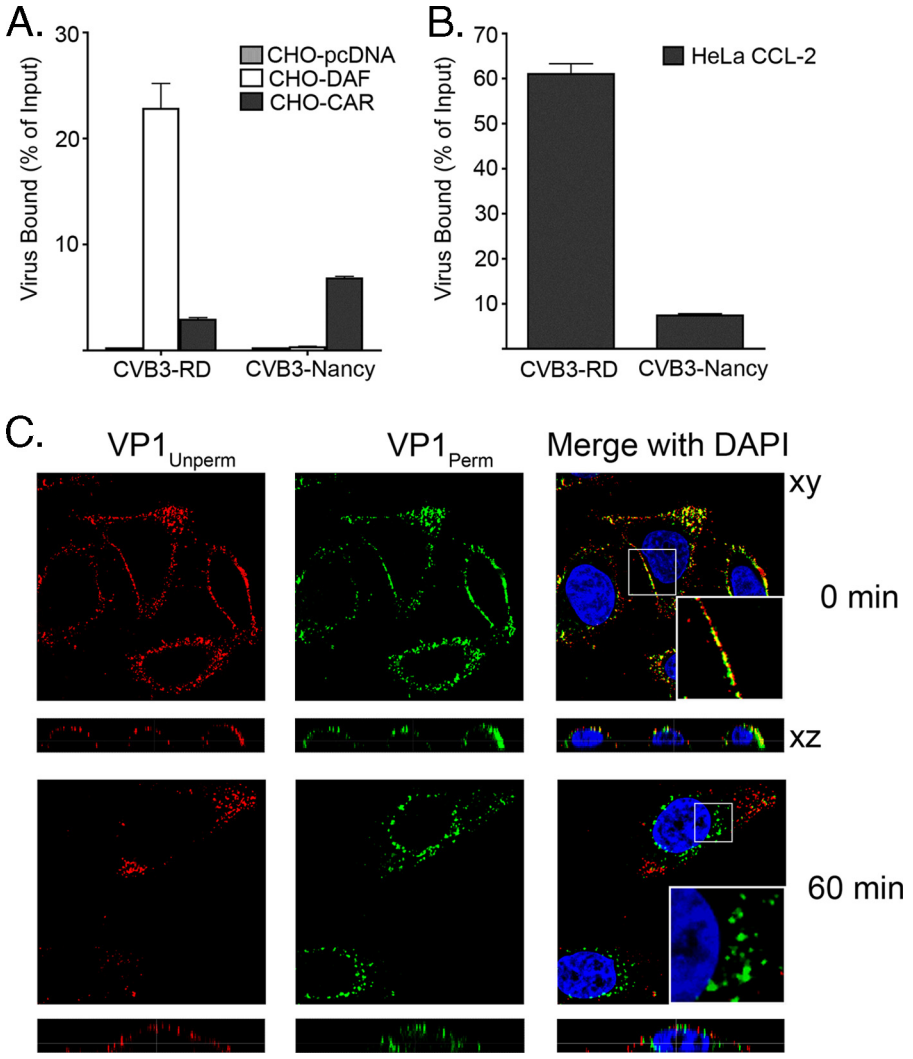

FIG. 1. CVB3 binding and entry. (A and B) ^{35}S-labeled CVB3-RD and CVB3-Nancy were bound to confluent CHO cells stably transfected with CAR, DAF, or vector alone (pcDNA) (A) or to HeLa CCL-2 cells (B) for 1 h at 16°C. Unbound virus was washed off, cells were lysed, and cell-bound radioactivity was measured. Data are presented as percentages of input virus bound to cells ± standard deviations for triplicate samples. (C) CVB3-RD (250 PFU/cell) was bound to HeLa CCL-2 cells, unbound virus was removed, and cells were placed at 37°C to permit virus internalization. Cells were serially stained for virus as described in Materials and Methods. Images were captured with a laser-scanning confocal microscope, using a 63× oil immersion objective. Virus was detected with a red fluorophore before permeabilization ($VP1_{Unperm}$) and with a green fluorophore after permeabilization ($VP1_{Perm}$). Red fluorescence (or overlapping red and green fluorescence) indicates virus on the cell surface; uniquely green fluorescence (absence of red) indicates internalized virus. Magnified inserts (×3) within merge panels demonstrate virus on the cell surface at 0 min but internalized by 60 min.

For VSV experiments, 1 PFU/cell was allowed to bind to cells for 1 h at 37°C, unbound virus was removed, complete medium was added, and virus was allowed to infect cells for 5 h. Infected cells were detected with anti-M protein antibody (clone 23H12), a kind gift from Ron Harty and Douglas Lyles (Wake Forest University).

Immunofluorescence microscopy and serial staining for virus entry. For all experiments, CVB was detected with anti-enterovirus VP1 and all staining was performed at room temperature. For infection experiments, cells were permeabilized during fixation with methanol:acetone. Anti-VP1 antibody was added for 1 h at a 1:200 dilution in PBS. After three short washes, secondary antibody was added for 30 min at a 1:500 dilution with 10% normal serum from the same source as the secondary antibody.

For entry experiments, a serial staining process was used to differentiate internalized virus from surface-associated virus (16). Cells were fixed with 4% PFA, which does not permeabilize cells, and surface-associated virus was detected with anti-VP1 antibody and an antimouse secondary antibody conjugated to a fluorophore (typically Alexa Fluor 546 or 405). Cells were refixed with 4% PFA, washed, treated with PBS-NH_4Cl, and permeabilized with 0.1% Triton X-100 for 10 min. Cells were blocked for 1 h with blocking buffer (0.01% saponin, 0.25% fish gelatin, and 0.02% sodium azide) and then incubated with the same anti-VP1 antibody (1:100 dilution in PBS) but with an antimouse secondary antibody conjugated to a different fluorophore (typically FITC or Alexa Fluor 546 if a FITC-conjugated antibody was used to detect another cellular protein). All costaining for cellular proteins was performed after permeabilization.

All slides were mounted with Vectaschield (Vector Laboratories). Infection images were captured with a BX51 Olympus fluorescence microscope (Melville, NY). Entry images were captured using a Leica TCS 4D laser-scanning confocal microscope using a 63× oil objective (Bannockburn, IL). For three-dimensional analysis, XZ- or YZ-series stacks were acquired at 0.6-μm intervals through the cell monolayer (8 to 10 μm thick).

Binding assays. CVB3-RD and CVB3-Nancy were radiolabeled with [^{35}S]methionine-cystine mixture as described elsewhere (7). ^{35}S-labeled virus (20,000 cpm per well) was bound to confluent CHO-CAR, CHO-DAF, or CHO-pcDNA cells in 24-well plates for 1 h at 16°C. Unbound virus was removed with three

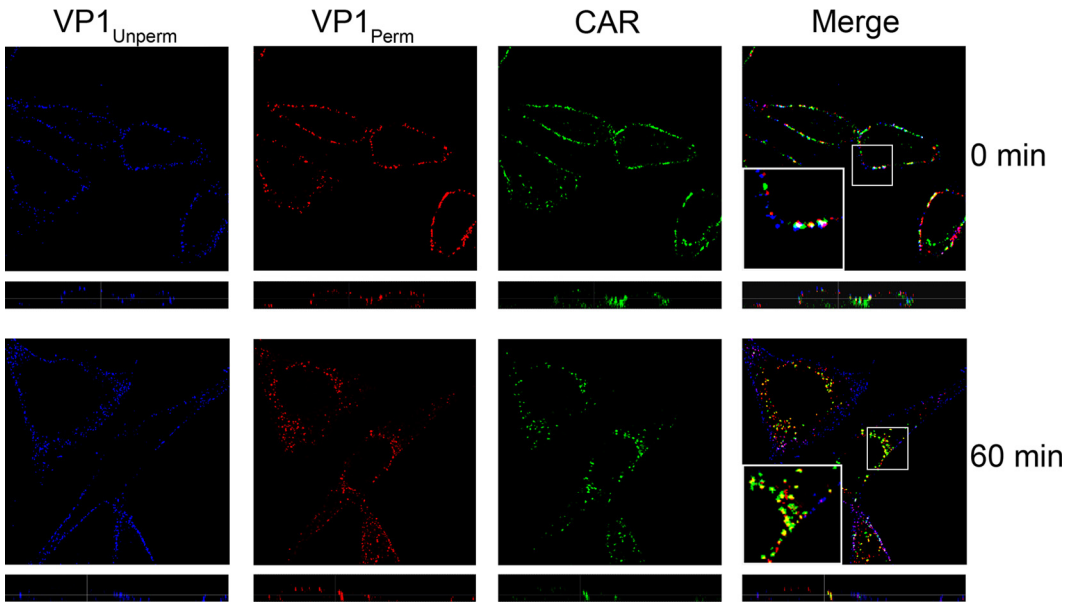

FIG. 2. CVB3-RD enters with CAR. CVB3-RD particles were bound to cells and allowed to enter for 60 min as in Fig. 1C. Virus was detected with a blue fluorophore before permeabilization ($VP1_{Unperm}$) and with a red fluorophore after permeabilization ($VP1_{Perm}$). Uniquely red fluorescence indicates internalized virus. CAR was stained with a green fluorophore after permeabilization. Images were captured with a laser-scanning confocal microscope using an oil immersion 63× objective. Inserts within merge panels are magnified 3×.

washes with binding buffer, cells were lysed with Solvable detergent (PerkinElmer, Waltham, MA), and cell-bound radioactivity was assessed.

Transferrin uptake assay. For all transferrin uptake experiments, cells were serum starved for 30 min prior to the start of the experiment. Cells were incubated with 10 μg/ml transferrin conjugated to Alexa Fluor 594 for 40 min at 37°C. Following the entry period, surface transferrin was stripped with two 5-min acid washes (0.2 N acetic acid, 0.5 M NaCl; pH = 2.5) at 4°C. Chambers were removed, and slides were submerged 10 times in ice-cold PBS and mounted using Vectashield. For quantification, three fields at 40× objective were captured per well and cells were scored for internalized transferrin based on the Alexa Fluor 594 signal (100 to 150 total cells).

Statistical analysis. Student's *t* test was used to determine statistical significance. All graphs represent means and standard deviations of normalized data points for duplicate or triplicate samples from each of three independent experiments ($n = 6$ or 9).

RESULTS

CVB3-RD but not CVB3-Nancy binds to DAF. We first verified that CVB3-RD bound to both DAF and CAR, while its parental strain, CVB3-Nancy, bound only CAR. As expected, when ^{35}S-labeled virus was incubated with CHO cells stably transfected with human DAF, human CAR, or vector alone, CVB3-RD bound to both CHO-DAF and CHO-CAR whereas CVB3-Nancy bound only to CHO-CAR cells (Fig. 1A).

CVB3-RD virus particles are internalized with CAR. To examine virus particle entry, we used a serial staining approach (described in more detail in Materials and Methods) to differentiate internalized virus particles from virus on the cell surface. We permitted CVB3-RD (250 PFU/cell) to bind to cells at 16°C, shifted cells to 37°C to initiate entry, and at various times after the temperature shift, fixed the cells with a nonpermeabilizing agent. Virus particles on the surface were detected before permeabilization with antibody to the viral capsid protein VP1 and secondary antibody conjugated to a red fluorophore ($VP1_{Unperm}$). Cells were then permeabilized to expose internalized particles and restained with anti-VP1 and secondary antibody conjugated to a green fluorophore ($VP1_{Perm}$). Thus, internalized virus particles, which could be stained only after permeabilization with the green fluorophore-conjugated antibody, appeared uniquely green and were typically distant from any red signal. Surface-associated virus particles, which could be stained both before and after permeabilization, appeared either red or yellow (Fig. 1C).

CVB3-RD was first detected within the cell at 30 to 45 min (data not shown). At 60 min, internalized virus particles were seen in most cells as uniquely green punctae, often near the nucleus; some virus remained on the cell surface (Fig. 1C). At later time points, virus particles were concentrated above the nucleus in many cells, although perinuclear virus was still observed (data not shown). In subsequent experiments, we assessed virus entry at 60 min, since we could reliably observe virus particles in the majority of cells at this time point.

CVB3-RD enters polarized Caco-2 cells without its major receptor CAR, which remains within the tight junction (15). In HeLa CCL-2 cells, we observed both CAR and CVB3-RD predominantly on the cell surface at 0 min; at 60 min, most of the CAR (green) was observed inside the cell, where it colocalized with internalized virus particles (red, $VP1_{Perm}$) (Fig. 2). This observation suggests that CAR enters these cells along with the virus.

We were not able to visualize CVB3-Nancy on the cell surface, most likely because the amount of bound virus was too small to detect by immunofluorescence. ^{35}S-labeled CVB3-Nancy bound to HeLa CCL-2 cells with much lower efficiency than did CVB3-RD (Fig. 1B), consistent with the previous observation that there are many fewer binding sites on HeLa cells for CVB3-Nancy than for CVB3-RD (23). In all further

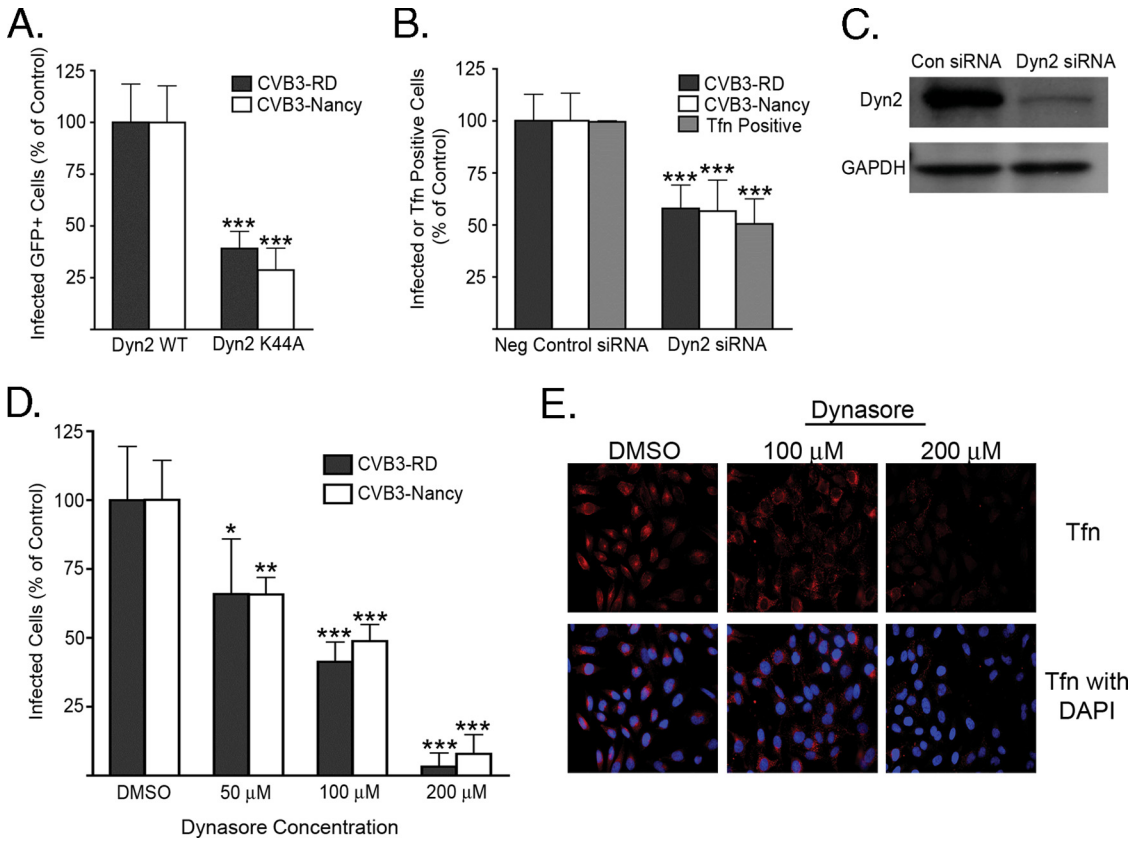

FIG. 3. Both CVB3 isolates require dynamin for infection. (A) Cells transiently transfected with plasmids expressing WT or K44A dynamin 2 (Dyn2 WT or Dyn2 K44A) were infected with CVB3-RD (5 PFU/cell) or CVB3-Nancy (30 PFU/cell). Infection was stopped at 6 h, and new viral protein was detected by staining. Infection was quantified as the percentage of transgene-positive cells that were positive for virus. (B) Cells serially transfected with siRNAs targeting dynamin 2 were infected with CVB3-RD or CVB3-Nancy. In parallel, cells were scored for transferrin (Tfn) uptake as described in Materials and Methods. Neg control, negative control. (C) Immunoblot of cell lysates after serial transfection with negative control (Con) or siRNAs targeting dynamin 2 (Dyn2). The GAPDH blot serves as a loading control. (D) Dynasore-treated cells were infected with CVB3-RD or CVB3-Nancy. Cells were pretreated with dynasore for 45 min, and drug was present throughout binding and for the first 3 h of infection. Complete medium with NuSerum instead of FBS was used. (E) Tfn uptake in dynasore-treated cells. Cells were treated with dynasore for 45 min at 37°C, followed by 1 h at 16°C (to match treatment of virus-infected samples). Alexa Fluor 594-Transferrin was then added to cells in complete medium with NuSerum and allowed to internalize for 40 min at 37°C. Images were captured with a 40× objective. For all infection graphs, data represent the normalized percentages of cells infected ± standard deviations for triplicate samples from each of three independent experiments, except for dynasore experiments, in which duplicate samples were used. *P* values: *, <0.05; **, <0.01; ***, <0.001.

experiments, both CVB3-RD and CVB3-Nancy were used for infection assays but only CVB3-RD was used to examine entry.

Infection depends on dynamin. Dynamin 2 is a GTPase required for the fission of vesicles in several endocytic pathways (20). We examined the importance of dynamin for CVB3 infection by use of a well-characterized DN dynamin mutant (K44A) (18, 42, 67) and by depletion of dynamin with siRNA. Cells transiently transfected with GFP-tagged WT or DN dynamin and cells serially transfected with pooled validated siRNAs targeting dynamin were exposed to CVB3-RD (5 PFU/cell) or CVB3-Nancy (30 PFU/cell). At 6 h, cells were fixed and stained with anti-VP1 to detect newly synthesized viral protein as a measure of infection. Cells transfected with DN dynamin or depleted of dynamin by siRNA were infected by both CVB3 isolates at a much lower frequency than cells transfected with WT dynamin or negative control siRNA (Fig. 3A and B). Transferrin uptake, which is known to require dynamin and clathrin (67), was inhibited, as expected, by both dynamin 2 K44A (data not shown) and dynamin depletion (Fig. 3B).

Because dynamin is required for a number of nonendocytic cellular functions (31, 38, 41), we used a rapidly acting reversible dynamin inhibitor, dynasore, to determine if dynamin was required early in infection (32). When cells were pretreated and kept in the presence of dynasore throughout virus binding and the first 3 h after initiation of infection, infection by both CVB3-RD and CVB3-Nancy was inhibited in a dose-dependent manner; at 200 μM, the inhibition was virtually complete (Fig. 3D). In a control experiment, dynasore had no effect on binding of ^{35}S-labeled virus (data not shown). Transferrin uptake was inhibited in a similar dose-dependent manner, with a complete block of transferrin uptake at 200 μM and a partial effect at 100 μM (Fig. 3E). Addition of dynasore at 3 h had a significantly smaller inhibitory effect on infection (data not shown). These results suggest that for both isolates, dynamin is required for a postattachment event early in infection.

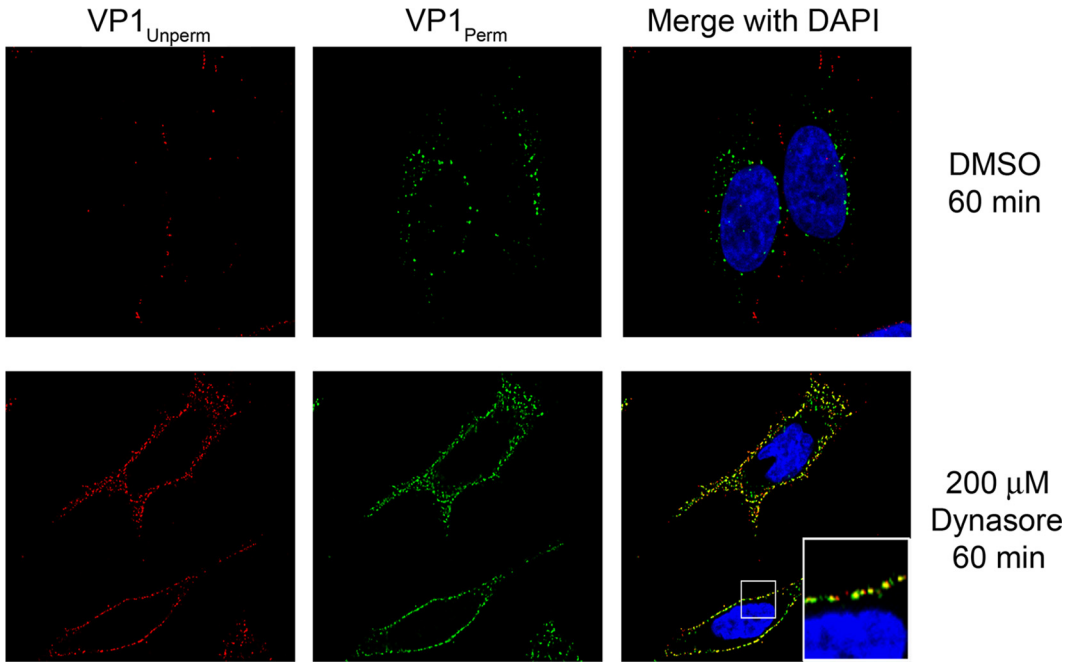

FIG. 4. CVB3-RD entry requires dynamin. CVB3-RD particles were bound to and allowed to enter cells pretreated with DMSO or 200 μM dynasore. Unbound virus was washed off, complete medium with NuSerum and dynasore was added, and virus was allowed to enter cells for 60 min. Virus was detected with a red fluorophore before permeabilization ($VP1_{Unperm}$) and with a green fluorophore after permeabilization ($VP1_{Perm}$). Uniquely green fluorescence indicates internalized virus. Images were captured with a laser-scanning confocal microscope using an oil immersion 63× objective. The magnified insert (×3) in the bottom merge panel demonstrates $VP1_{Perm}$ signal significantly colocalizes with $VP1_{Unperm}$ signal and no uniquely green signal is present near the nucleus.

Dynamin is required for entry. We next determined whether dynamin inhibition blocked virus particle entry rather than another early event. We pretreated cells with dynasore or DMSO carrier, exposed them to CVB3-RD, and examined virus particle uptake at 60 min. In control cells, virus was observed primarily as green punctae near the nucleus (Fig. 4, top panels). However, in dynasore-treated cells, virus was trapped on the surface and restricted to the cell periphery, as demonstrated by the extensive colocalization of red (unpermeabilized) and green signals (permeabilized) (Fig. 4, bottom panels). A similar block to virus entry was observed in cells transfected with dynamin 2 K44A (data not shown). Thus, we show for the first time that dynamin inhibition blocks CVB3 entry as well as infection. This result also indicates that infection requires the uptake of virions into the cells and is not consistent with a model of entry in which viral genomes enter the cell directly from the surface.

Infection does not require clathrin or endosomal acidification. Clathrin-dependent endocytosis is the best-characterized dynamin-requiring pathway. Cargoes internalized by clathrin, as well as other pathways, are delivered to the endosomal system, and some viruses require endosomal acidification to complete the entry process. Both clathrin endocytosis and acidification had previously been implicated in CVB3 infection of HeLa cells (13); however, we wanted to test this using more-specific reagents.

We tested the importance of clathrin endocytosis by using CPZ, a drug commonly used to inhibit clathrin pathways, and siRNAs targeting clathrin heavy chain. A small decrease in infection by both CVB3-RD and CVB3-Nancy was seen when cells were treated with CPZ (Fig. 5A), but the effect was not dose dependent. In contrast to its slight effect on virus infection, CPZ had a marked dose-dependent effect on transferrin uptake (Fig. 5A). We also observed a decrease in binding of ^{35}S-labeled virus to CPZ-treated cells (data not shown), suggesting that the decreased infection might reflect a decrease in virus attachment rather than internalization. These results suggested that virus infection did not depend on clathrin-mediated endocytosis.

Consistent with this conclusion, depletion of clathrin heavy chain, an essential component of the clathrin-coated vesicle (21, 40), had no effect on infection by either CVB3 isolate but markedly decreased transferrin uptake; 50% of clathrin heavy chain siRNA-transfected cells showed no internalized transferrin (Fig. 5B and C). We examined virus entry and transferrin uptake simultaneously in cells depleted of clathrin heavy chain; even in the cells with no transferrin uptake (i.e., those with most-effective depletion of clathrin), internalized virus was clearly evident (data not shown). Further, depletion of alpha-adaptin, an adaptor molecule important for internalization of many clathrin cargoes (40), did not reduce infection despite blocking transferrin uptake (data not shown). Thus, in contrast to the conclusion of other investigators (13), our data obtained using more clathrin-specific inhibitors indicate that CVB3 infection of HeLa cells does not require clathrin endocytosis.

We used NH_4Cl (a lysosomotropic agent) and bafilomycin (an endosomal Na/H^+ pump inhibitor) to prevent endosomal acidification. At concentrations that blocked infection by VSV, a virus known to depend on acidification (63), neither agent

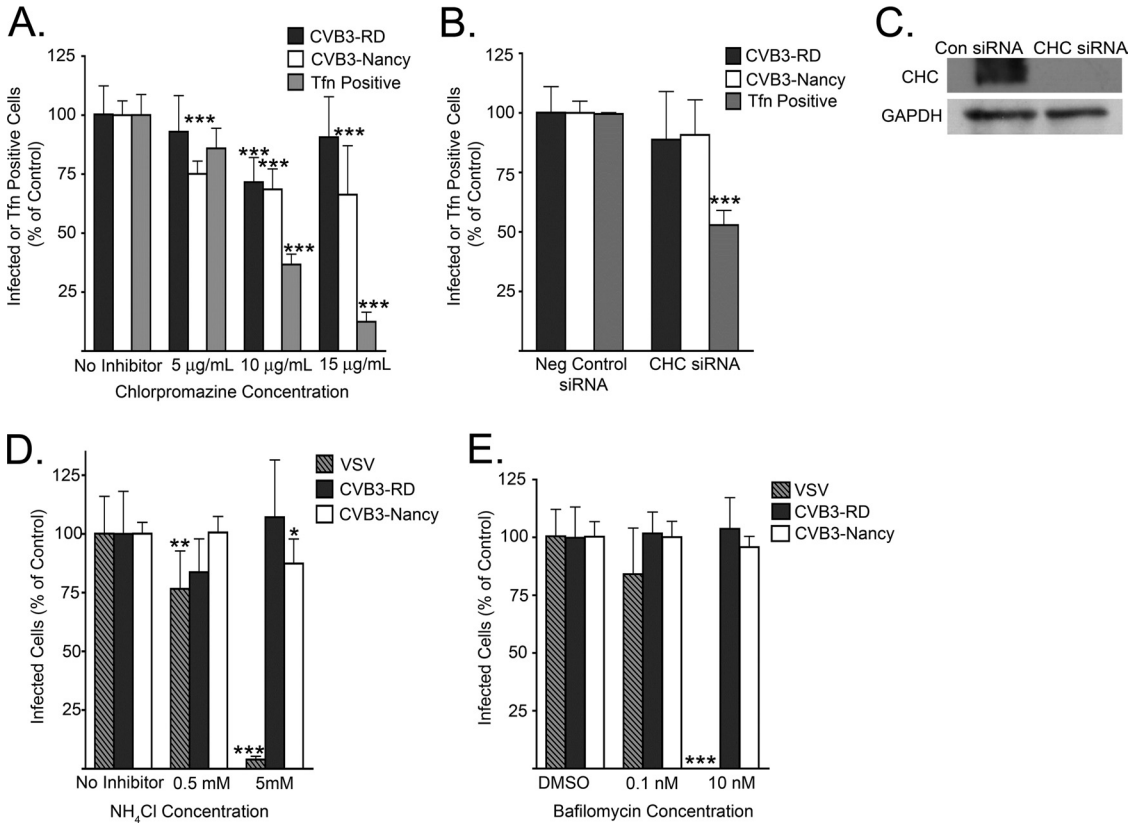

FIG. 5. Clathrin and endosomal acidification are not required for infection. (A and B) Cells treated with CPZ (A) or depleted of clathrin heavy chain by serial transfection with siRNAs (B) were infected with CVB3-RD or CVB3-Nancy. In parallel, transferrin (Tfn) uptake was assessed. Cells were pretreated with CPZ for 1 h, and drug was present throughout binding and infection. (C) Immunoblot of cell lysates after serial transfection with negative control (Con) or siRNAs targeting clathrin heavy chain (CHC). GAPDH was used as a loading control. (D and E) Cells were treated with endosomal acidification inhibitor NH_4Cl (D) or bafilomycin A1 (E) and then infected with CVB3-RD, CVB3-Nancy, or VSV (an acidification-dependent virus). Cells were pretreated for 1 h, and drugs were present throughout binding and infection. For all infection graphs, data represent the normalized percentages of cells infected ± standard deviations for duplicate samples from each of three independent experiments, except for clathrin heavy chain siRNA experiments, in which triplicate samples were used. Transferrin uptake data for CPZ-treated cells were from a representative experiment in which four fields (each with 30 to 50 cells) from two wells were counted for each condition. *P* values: *, <0.05; **, <0.01; ***, <0.001.

inhibited infection by either CVB3 isolate (Fig. 5D and E). These results suggest that acidification is not required for infection by CVB3-RD or CVB3-Nancy.

Caveolin depletion does not inhibit infection. Another well-studied dynamin-dependent pathway is caveolar endocytosis. Caveolin associates with lipid rafts to form caveolae, through which a number of cargoes are internalized (15, 42). Dynamin is typically required for internalization of caveolae (42). Caveolin is also required for dynamin-independent uptake of CVB3-RD in Caco-2 cells (15).

HeLa CCL-2 cells express both Cav-1 and Cav-2. Cav-1 is the functional caveolin found within caveolae (51). Cav-1 and Cav-2 are expressed in the same cell types and are known to oligomerize, although Cav-2 does not have a known role in caveolar endocytosis (46, 54). Serial transfections with pooled validated siRNAs targeting Cav-1 and Cav-2 led to a robust reduction of total caveolin (Fig. 6B). When transfected cells were exposed to either isolate, no substantial reduction in infection was observed (Fig. 6A). We also tested the effect on infection of a previously characterized DN caveolin (Cav DN) (15, 47, 59). Cells transfected with Cav DN were infected by both isolates at the same frequencies as were cells transfected with WT caveolin (Fig. 6C). In a control experiment (data not shown), Cav DN inhibited CVB3-RD infection of Caco-2 cells, as we had previously observed (15).

We were unable to demonstrate that perturbations of caveolin function blocked internalization of described caveolin-dependent cargoes—simian virus 40 (SV40) and cholera toxin B subunit (CTB)—in HeLa CCL-2 cells (data not shown). We found that HeLa CCL-2 cells resisted SV40 infection and did not bind CTB, most likely because they lack GM1 ganglioside, the receptor for both of these ligands (45, 66). We were able to restore binding of CTB and susceptibility to SV40 by treating cells with exogenous GM1. However, we were still unable to inhibit CTB uptake or SV40 infection (data not shown). These cargoes depend on caveolin for entry in some cell types (1, 43, 47, 57) but may use noncaveolar pathways as well (19, 36, 45, 57, 64). In particular, CTB entry has been seen to occur by a noncaveolar mechanism in HeLa cells with low levels of endogenous caveolin (57), suggesting a noncaveolin pathway may allow for CTB internalization in HeLa CCL-2 cells after depletion or inhibition of caveolin. Also, the addition of exoge-

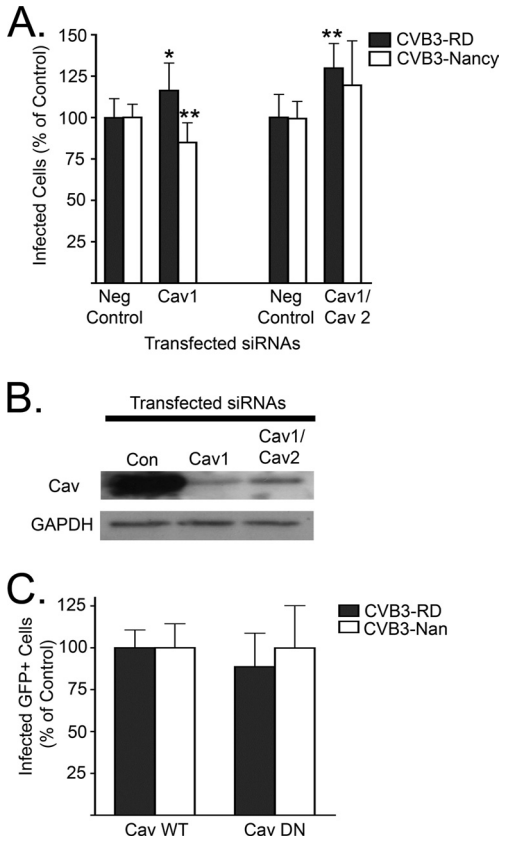

FIG. 6. Caveolin depletion does not inhibit infection. (A) Cells depleted of Cav-1 alone or both Cav-1 and Cav-2 by serial siRNA transfections were infected with CVB3-RD or CVB3-Nancy. Neg control, negative control. (B) Immunoblot of cell lysates following transfection with negative control (Con), Cav-1, or Cav-1 and Cav-2 targeting siRNAs. (C) Cells transfected with WT caveolin (Cav WT) or Cav DN were infected with CVB3-RD or CVB3-Nancy. Only transgene-positive cells were counted to determine the infection percentage. For all infection graphs, data represent the normalized percentages of cells infected ± standard deviations for triplicate samples from each of three independent experiments. *P* values: *, <0.05; **, <0.01.

nous GM1 has been demonstrated to alter the internalization mechanism of GM1 bound to CTB in HeLa cells (57), suggesting that in some cell types, GM1 ligands may enter by different pathways if they are bound to exogenous GM1 as opposed to endogenous GM1.

Because of our inability to block uptake of cargo that can use caveolar endocytosis, we cannot definitively exclude a role for caveolar endocytosis in CVB3 entry into HeLa CCL-2 cells. However, given the magnitude of caveolin depletion by siRNAs and the efficacy of Cav DN in other nonpolarized and polarized cells (8, 15, 16, 59), as well as previous reports demonstrating that caveolar cargoes SV40 and CTB may use noncaveolar pathways, we think our data support the conclusion that CVB3 entry does not require clathrin or caveolin.

Lipid rafts are required for infection and entry. Dynamin-dependent but clathrin- and caveolin-independent endocytic pathways have been described previously, and many of these require cholesterol-rich lipid rafts for their function (20, 34). We used two different drugs that act upon cholesterol to disrupt lipid rafts; both have been used to study lipid rafts in virus entry. Filipin forms a complex with cholesterol in the plasma membrane (11, 26, 58), whereas MβCD extracts cholesterol from the plasma membrane (24).

When cells were pretreated with 1 μg/ml filipin and kept in the presence of drug throughout virus binding and the first 3 h following infection initiation, infection by both CVB3-RD and CVB3-Nancy was inhibited (Fig. 7A). The inhibitory effect did not result from a loss of membrane integrity, as demonstrated by exclusion of propidium iodide by cells treated with 1 μg/ml filipin (data not shown). When filipin was added at 3 h after initiation of infection, there was no reduction of infection, indicating that filipin acted early in the virus life cycle (Fig. 7B).

Consistent with the results obtained with filipin, infection by both CVB3-RD and CVB3-Nancy was inhibited in cells pretreated with 5 mM MβCD (Fig. 7C). When cholesterol was added back to the cells after MβCD treatment but prior to virus binding, no inhibition was seen. Further, treatment of cells with MβCD at 3 h after infection initiation had no inhibitory effect on infection by either virus, again suggesting that lipid rafts were needed early in infection. Both drugs acted specifically on raft-dependent pathways, since neither filipin nor MβCD had an inhibitory effect on transferrin uptake (data not shown) and MβCD treatment did not reduce infection by VSV (Fig. 7C), a virus that uses raft-independent clathrin-mediated endocytosis to infect cells (62).

To test whether intact lipid rafts were required for virus particle entry, we treated cells with filipin or MβCD. In both cases, virus particles were trapped on the cell surface at 60 min, as demonstrated by the extensive colocalization of red (prepermeabilized) and green (permeabilized) signal on the edge of the cell (Fig. 8, second and fourth rows). Addition of cholesterol following MβCD treatment reversed the inhibitor effect of MβCD on particle entry, and virus could be clearly seen in a perinuclear location at 60 min (Fig. 8, third row). Thus, both CVB3-RD and CVB3-Nancy require intact lipid rafts in addition to dynamin for entry and infection in HeLa CCL-2 cells.

Potential kinase involvement early in infection. CVB3-RD infection of polarized Caco-2 cells requires activation of tyrosine kinases, specifically Abl and Fyn (15). We used imatinib, a specific Abl inhibitor, and genistein, a tyrosine kinase inhibitor with broad specificity, to test the role of tyrosine kinases in CVB3 infection of HeLa CCL-2 cells. Imatinib treatment had no effect on infection by either virus isolate (Fig. 9A); however, in a control experiment, imatinib inhibited CVB3-RD infection of Caco-2 cells by more than 50% (data not shown). Genistein treatment inhibited infection of HeLa CCL-2 cells by both viruses but only when present at the start of infection (Fig. 9B). When genistein was added at 1 h or later, the inhibitory effect was markedly reduced (Fig. 9B). These results suggest a role for some tyrosine kinase, but not Abl, early in infection.

Given that genistein blocks entry of a number of viruses, including CVB3-RD entry into Caco-2 cells (9, 15, 48), the early effect of genistein on infection led us to expect that genistein would trap CVB3-RD particles on the cell surface, as we had observed with the dynamin inhibitor dynasore and raft disruptors filipin and MβCD (Fig. 4 and 8). Surprisingly, this is not what we observed. At 60 min, although there appeared to be fewer internalized virus particles in genistein-treated cells

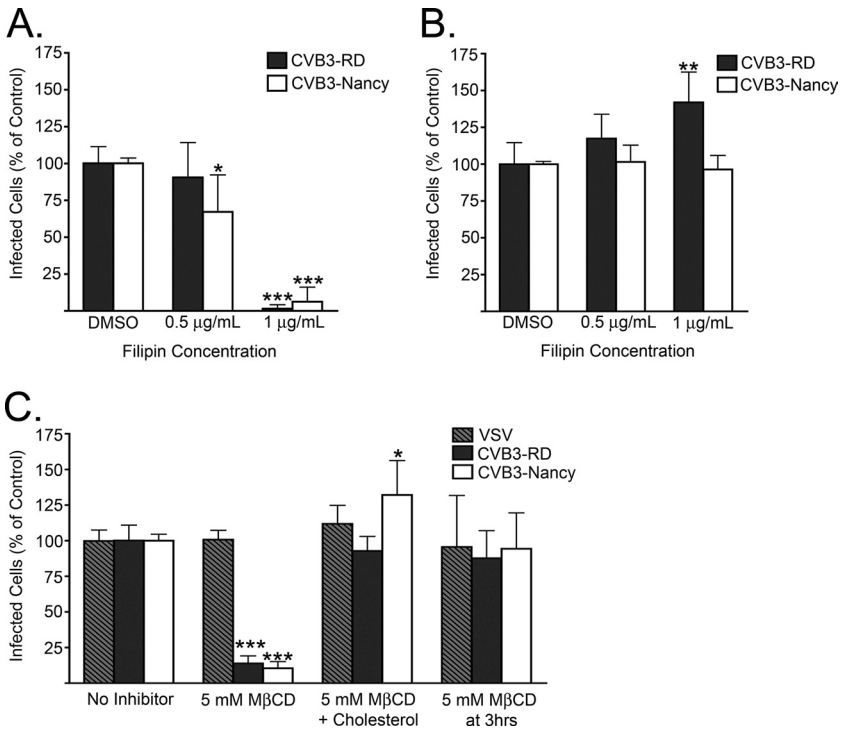

FIG. 7. Filipin and MβCD block infection. (A and B) Infection of filipin-treated cells. (A) Cells were treated with filipin for 45 min prior to binding by CVB3-RD and CVB3-Nancy, and drug was present throughout binding and for the first 3 h following infection initiation. (B) Filipin was added at 3 h after initiation of infection. (C) Infection of MβCD- or MβCD and cholesterol-treated cells. Cells were treated with 5 mM MβCD for 45 min, followed by an hour's treatment with 0.25 mM water-soluble cholesterol (MβCD + Cholesterol) or complete medium with NuSerum alone (MβCD). CVB3-RD, CVB3-Nancy, and VSV (a raft-independent pathway using virus) were then bound to cells, and infection occurred without drug present. For cells that received MβCD treatment at 3 h, medium with 5 mM MβCD was added to cells for 45 min and then replaced with complete medium with NuSerum alone. For all infection graphs, data represent the normalized percentages of cells infected ± standard deviations for duplicate samples from each of three independent experiments. *P* values: *, <0.05; **, <0.01; ***, <0.001.

than in control cells, uniquely green punctae were clearly visible in most cells (Fig. 9C, top two rows, arrows and insert). At a later time point (120 min), there was no difference in the appearance of internalized virus in genistein-treated and control cells (Fig. 9C, bottom two rows). Taken together, the results with kinase inhibitors suggest that tyrosine kinases are important for an early event in virus infection, although they do not appear to be essential for internalization of viral particles.

DISCUSSION

In this study, we examined how CVB3 enters nonpolarized HeLa CCL-2 cells and whether DAF-binding capacity affects this entry process. Inhibition of dynamin and disruption of lipid rafts blocked infection by both DAF-binding CVB3-RD and non-DAF-binding CVB3-Nancy. The same inhibitors that blocked infection also blocked the internalization of CVB3-RD virus particles into cells. Inhibition of clathrin-mediated endocytosis or endosomal acidification, as well as depletion of caveolin and Cav DN, had no effect on infection by either isolate. Taken together, our results indicate that both isolates require dynamin and lipid rafts to enter and infect HeLa CCL-2 cells and suggest that interaction with DAF does not change the entry pathway.

The virus entry pathway we characterized in HeLa CCL-2 cells differs significantly from the caveolin-dependent and dynamin-independent pathway by which CVB3-RD enters polarized Caco-2 cells (15, 17). Because CVB3-RD was used to characterize entry in both cell lines, the differences in the entry mechanism cannot be attributed to strain variation. Our results are consistent with a growing body of evidence that a single virus may use different mechanisms to infect different cell types (2, 19, 70). If viruses use multiple entry mechanisms, it may prove difficult to target entry mechanisms for antiviral therapy. It remains to be determined whether the Caco-2 entry pathway is used for infection of polarized cells in general and whether the HeLa CCL-2 entry pathway is used for infection of other nonpolarized cell types.

Our observations are consistent with reports by other investigators that dynamin is required for CVB3 infection (13, 33). Further, the results demonstrate that dynamin is specifically required for internalization of virus particles, an important clarification given that dynamin has nonendocytic cellular functions. Our results do not support the previously reported idea that CVB3 depends on clathrin or endosomal acidification for infection (13). The difference between our observation and those of other investigators may be explained by differences in CVB3 strains used or by differences in HeLa cell lines carried in different laboratories. However, we believe that technical differences are also important. Chung and colleagues (13) observed that infection was inhibited by siRNA depletion of Hsc70, a chaperone protein involved in uncoating of clathrin-

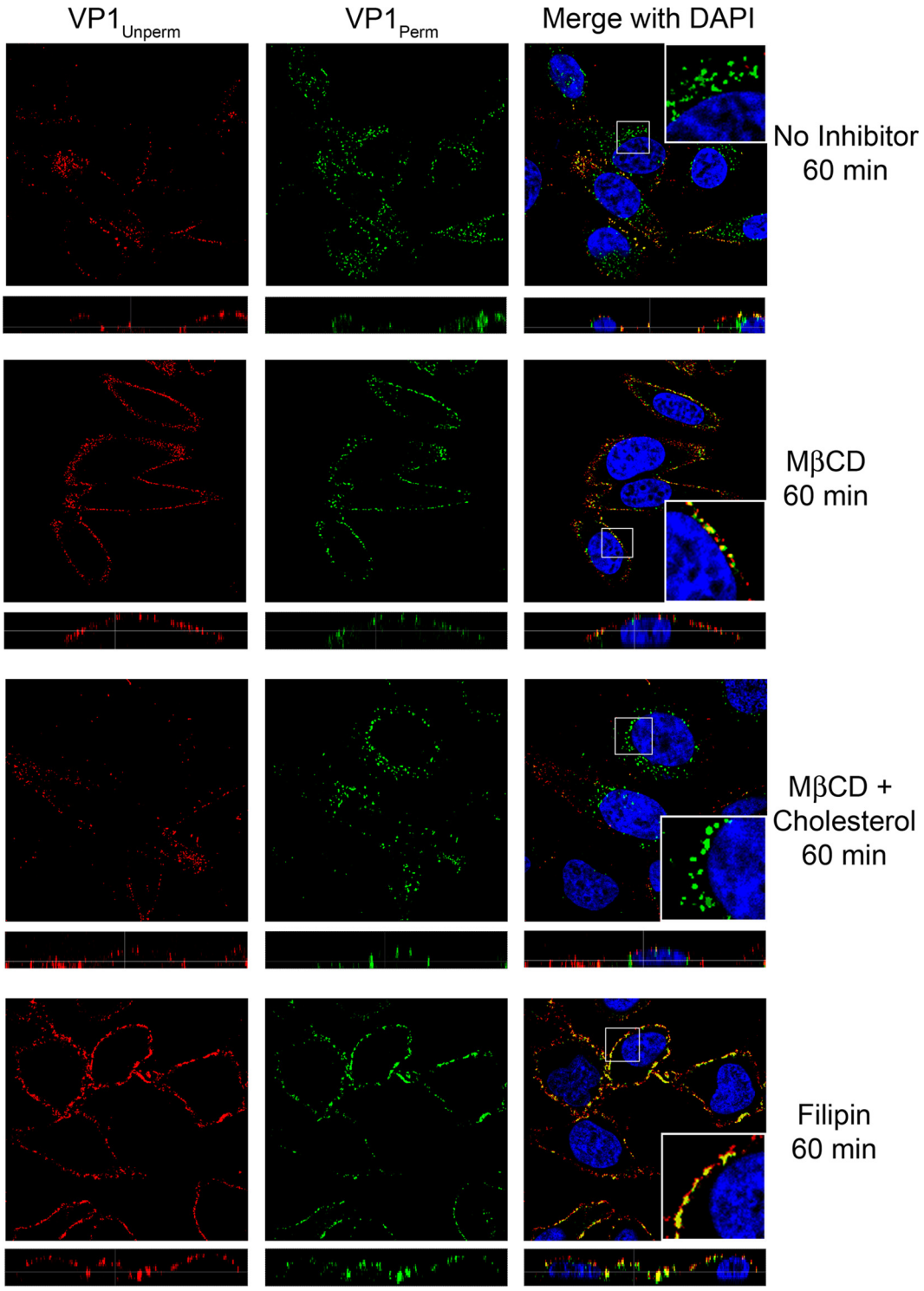

FIG. 8. Virus particle entry is blocked by filipin and MβCD. CVB3-RD particles were bound to and allowed to enter cells pretreated with medium alone, 5 mM MβCD, 5 mM MβCD plus cholesterol rescue, or 1 μg/ml filipin. For MβCD with cholesterol rescue cells, cells were treated with 0.25 mM cholesterol for 1 h after MβCD treatment and before virus binding. Only filipin-treated cells had drug present during virus binding. Unbound virus was washed off, complete medium with NuSerum and filipin or complete medium with NuSerum alone (MβCD, MβCD + Cholesterol) was added, and virus was allowed to enter cells for 60 min. Virus was detected with a red fluorophore before permeabilization ($VP1_{Unperm}$) and with a green fluorophore after permeabilization ($VP1_{Perm}$). Uniquely green fluorescence indicates internalized virus. Images were captured with a laser-scanning confocal microscope using an oil immersion 63× objective. Inserts within merge panels are magnified 3×.

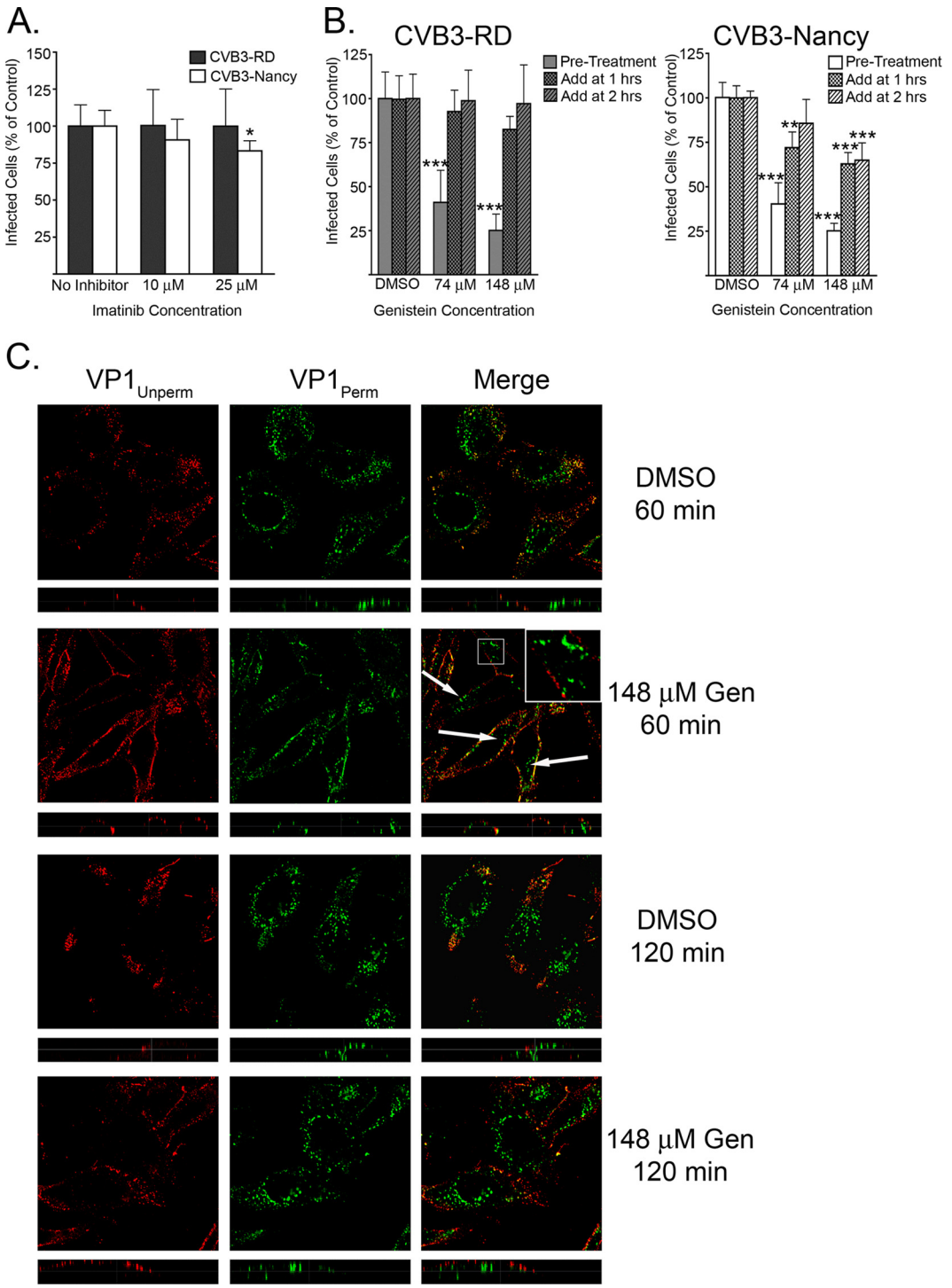

FIG. 9. Tyrosine kinases are involved early in infection but not in internalization. (A) Imatinib-treated cells were infected with CVB3-RD or CVB3-Nancy. Cells were treated with imatinib for 1 h prior to binding, and drug was present throughout binding and infection. (B) Genistein-treated cells were infected with CVB3-RD (left graph) or CVB3-Nancy (right graph). Three conditions were tested. For condition 1, cells were treated with genistein for 1 h prior to binding, with drug present throughout binding and the first 3 h of infection (Pre-Treatment). For condition 2, genistein was added 1 h after the start of infection (Add at 1 h). For condition 3, genistein was added 2 h after the start of infection (Add at 2 h). For conditions 2 and 3, drug remained for the duration of infection. For all infection graphs, data represent the normalized percentages of cells infected ± standard deviations for duplicate samples from each of three independent experiments. (C) CVB3-RD particles were bound to and allowed to enter cells pretreated with DMSO or 148 μM genistein. Unbound virus was washed off, complete medium with genistein (Gen) was added, and virus was allowed to enter cells for 60 or 120 min. Virus was detected with a red fluorophore before permeabilization ($VP1_{Unperm}$) and with a green fluorophore after permeabilization ($VP1_{Perm}$). Uniquely green fluorescence indicates internalized virus. Arrows and insert identify internalized virus particles within genistein-treated cells at 60 min. Images were captured with a laser-scanning confocal microscope using an oil immersion 63× objective. Inserts within merge panels are magnified 3×. *P* values: *, <0.05; **, < 0.01; ***, < 0.001.

coated vesicles. However, Hsc70 is also important for many other cellular functions, including protein folding, degradation, and transport across membranes (reviewed in reference 37). It has been reported to affect multiple events in virus infection, including transport of adenovirus DNA into the nucleus, assembly of the polyomavirus capsid, and disassembly of the reovirus capsid during entry (12, 27, 53).

We targeted clathrin endocytosis in a more specific manner by depleting cells of clathrin heavy chain, a protein required for formation of clathrin vesicles, and observed no effect on infection. In cells depleted of clathrin heavy chain that could not internalize transferrin (i.e., functionally deficient in clathrin endocytosis), internalized virus particles were still observed, suggesting that virus entry, in addition to infection, is not effected by clathrin inhibition. We also found that depletion of the clathrin adaptor protein alpha-adaptin had no effect on infection and CPZ had only a slight effect, which correlated with a decrease in binding of virus to the cell. The previous study also found that CVB3 infection was blocked by 50 mM NH_4Cl, a concentration that is much higher than required to block infection by many acidification-dependent viruses (14, 29, 61, 63). We saw no inhibition of CVB3 infection by 5 mM NH_4Cl or 10 nM bafilomycin, both of which completely blocked VSV infection. Taken together, our results with more-specific inhibitors of clathrin endocytosis and endosomal acidification demonstrate that there is no requirement for either process in CVB3 entry and infection of HeLa CCL-2 cells.

The dynamin-dependent pathway that CVB3-RD and CVB3-Nancy use to enter HeLa CCL-2 cells also depends on membrane cholesterol and most likely lipid rafts. Many investigators consider caveolar endocytosis to be a subset of the endocytic pathways dependent on lipid rafts. We were unable to confirm that caveolin depletion or Cav DN blocked internalization of SV40 or cholera toxin B subunit in HeLa CCL2 cells supplemented with the GM1 receptor. In the absence of a robust positive control, we cannot definitively exclude a role for caveolin in CVB3 entry. However, these ligands have been reported to enter by noncaveolar routes in some cells (19, 36, 45, 57, 64), including some HeLa cells, and our results provide no evidence that caveolin is necessary. Entry by CVB3 may occur by recently described dynamin- and lipid raft-dependent but caveolin- and clathrin-independent pathways, such as those responsible for internalization of interleukin 2 receptor (30), rotavirus (52), and feline infectious peritonitis virus (68). Additional studies are required to understand and define the molecular components of these pathways, and CVB3 may serve as a model ligand.

We used two closely related CVB3 strains that differed in their DAF-binding capacity to examine the role of DAF in CVB3 entry into nonpolarized cells. Although we were unable to directly observe the entry of CVB3-Nancy particles, endocytic inhibitors that blocked CVB3-RD particle entry had the same effects on infection by both CVB3-RD and CVB3-Nancy, suggesting that the entry pathways for the two isolates are the same. Despite evidence that interaction with specific surface proteins can influence virus entry mechanisms (2, 60), these results suggest that DAF binding does not alter the way CVB3 enters HeLa CCL-2 cells.

We observed that virus and CAR colocalized within the cell, suggesting that they enter and traffic together. CAR induces conformational changes in the viral capsid that are believed to be necessary for release of the RNA genome. We found that inhibition of dynamin activity, as well as disruption of lipid rafts, blocked virus infection and trapped virus particles at the cell surface; these results suggest that genome release does not occur until viral particles have been internalized. We do not know whether virus is directly bound to CAR as it enters the cell, but the proximity of CAR and virus in intracellular compartments suggests that CAR may be well situated to trigger genome release within the cell.

Because tyrosine kinase signals are critical for CVB3 entry into Caco-2 cells, we examined the effects of tyrosine kinase inhibitors on entry into HeLa CCL-2 cells. Abl kinase is required for the infection of Caco-2 cells because Abl-mediated rearrangements of the cell surface are needed for virus to come into contact with CAR in the tight junction. In HeLa cells, where both CAR and DAF are accessible on the cell surface, we found that inhibition of Abl by imatinib had no effect on infection. Additional tyrosine kinase signals are also essential in Caco-2 cells for caveolin-dependent virus internalization. We found that genistein, a broad-spectrum inhibitor of protein tyrosine kinases, inhibited an early step in infection in HeLa CCL-2 cells. However, unlike dynasore, filipin, and MβCD, which trapped virus on the cell surface, genistein did not block entry of virus particles. This suggests that tyrosine kinases may be required for other early events in infection, such as virus trafficking to an appropriate intracellular compartment or the release of the genome into the cell. Analysis of kinases and other signaling molecules required for these early events may be highly informative about nonendocytic processes coopted by viruses.

Viruses use normal cellular processes to accomplish each step in their life cycle. These processes may be subtly different in different cell types, presenting viruses with distinctive environments in which to make their way. To initiate infection in any cell, a virus must bind to a receptor, move into the cell, and release its genome at an appropriate time and place. It is not clear why CVB3 use one mechanism to enter HeLa cells and another to enter Caco-2 cells, but it is likely that the entry process in each cell type reflects a different solution to the same problem. Learning more about the subtle differences that lead viruses to enter cells in different ways will teach us about both the viruses and the endocytic processes upon which they rely.

ACKNOWLEDGMENTS

This work was supported by grants from the NIH (R01AI072490 and T32AI007324).

We are grateful to Ari Helenius, Lucas Pelkmans, Mark McNiven, Ron Harty, and Douglas Lyles for the kind gift of reagents and Tom Kirchhausen and Keith Soloman for technical advice regarding dynasore and filipin, respectively. Confocal images were acquired with the assistance of Edward Williamson and the confocal core facility at the Joseph Stokes Research Institute at the Children's Hospital of Philadelphia. We thank Lili Zhang for technical assistance and ChonSaeng Kim, Nicole LeLay, and Jason Newland for helpful discussions and comments on the manuscript.

REFERENCES

1. **Anderson, H. A., Y. Chen, and L. C. Norkin.** 1996. Bound simian virus 40 translocates to caveolin-enriched membrane domains, and its entry is inhibited by drugs that selectively disrupt caveolae. Mol. Biol. Cell **7:**1825–1834.

2. **Bengali, Z., A. C. Townsley, and B. Moss.** 2009. Vaccinia virus strain differences in cell attachment and entry. Virology **389:**132–140.
3. **Bergelson, J. M., M. Chan, K. R. Solomon, N. F. St John, H. Lin, and R. W. Finberg.** 1994. Decay-accelerating factor (CD55), a glycosylphosphatidylinositol-anchored complement regulatory protein, is a receptor for several echoviruses. Proc. Natl. Acad. Sci. USA **91:**6245–6248.
4. **Bergelson, J. M., J. A. Cunningham, G. Droguett, E. A. Kurt-Jones, A. Krithivas, J. S. Hong, M. S. Horwitz, R. L. Crowell, and R. W. Finberg.** 1997. Isolation of a common receptor for coxsackie B viruses and adenoviruses 2 and 5. Science **275:**1320–1323.
5. **Bergelson, J. M., J. F. Modlin, W. Wieland-Alter, J. A. Cunningham, R. L. Crowell, and R. W. Finberg.** 1997. Clinical coxsackievirus B isolates differ from laboratory strains in their interaction with two cell surface receptors. J. Infect. Dis. **175:**697–700.
6. **Bergelson, J. M., J. G. Mohanty, R. L. Crowell, N. F. St John, D. M. Lublin, and R. W. Finberg.** 1995. Coxsackievirus B3 adapted to growth in RD cells binds to decay-accelerating factor (CD55). J. Virol. **69:**1903–1906.
7. **Bergelson, J. M., N. St John, S. Kawaguchi, M. Chan, H. Stubdal, J. Modlin, and R. W. Finberg.** 1993. Infection by echoviruses 1 and 8 depends on the alpha 2 subunit of human VLA-2. J. Virol. **67:**6847–6852.
8. **Bradley, C. A., C. Taghibiglou, G. L. Collingridge, and Y. T. Wang.** 2008. Mechanisms involved in the reduction of GABAA receptor α1-subunit expression caused by the epilepsy mutation A322D in the trafficking-competent receptor. J. Biol. Chem. **283:**22043–22050.
9. **Brandenburg, B., L. Y. Lee, M. Lakadamyali, M. J. Rust, X. Zhuang, and J. M. Hogle.** 2007. Imaging poliovirus entry in live cells. PLoS Biol. **5:**e183.
10. **Cao, H., H. M. Thompson, E. W. Krueger, and M. A. McNiven.** 2000. Disruption of Golgi structure and function in mammalian cells expressing a mutant dynamin. J. Cell Sci. **113:**1993–2002.
11. **Carter, G. C., L. Bernstone, D. Sangani, J. W. Bee, T. Harder, and W. James.** 2009. HIV entry in macrophages is dependent on intact lipid rafts. Virology **386:**192–202.
12. **Chromy, L. R., J. M. Pipas, and R. L. Garcea.** 2003. Chaperone-mediated in vitro assembly of polyomavirus capsids. Proc. Natl. Acad. Sci. USA **100:** 10477–10482.
13. **Chung, S. K., J. Y. Kim, I. B. Kim, S. I. Park, K. H. Paek, and J. H. Nam.** 2005. Internalization and trafficking mechanisms of coxsackievirus B3 in HeLa cells. Virology **333:**31–40.
14. **Clark, K. M., J. D. Wetzel, Y. Gu, D. H. Ebert, S. A. McAbee, E. K. Stoneman, G. S. Baer, Y. Zhu, G. J. Wilson, B. V. Prasad, and T. S. Dermody.** 2006. Reovirus variants selected for resistance to ammonium chloride have mutations in viral outer-capsid protein σ3. J. Virol. **80:**671–681.
15. **Coyne, C. B., and J. M. Bergelson.** 2006. Virus-induced Abl and Fyn kinase signals permit coxsackievirus entry through epithelial tight junctions. Cell **124:**119–131.
16. **Coyne, C. B., K. S. Kim, and J. M. Bergelson.** 2007. Poliovirus entry into human brain microvascular cells requires receptor-induced activation of SHP-2. EMBO J. **26:**4016–4028.
17. **Coyne, C. B., L. Shen, J. R. Turner, and J. M. Bergelson.** 2007. Coxsackievirus entry across epithelial tight junctions requires occludin and the small GTPases Rab34 and Rab5. Cell Host Microbe **2:**181–192.
18. **Damke, H., T. Baba, D. E. Warnock, and S. L. Schmid.** 1994. Induction of mutant dynamin specifically blocks endocytic coated vesicle formation. J. Cell Biol. **127:**915–934.
19. **Damm, E. M., L. Pelkmans, J. Kartenbeck, A. Mezzacasa, T. Kurzchalia, and A. Helenius.** 2005. Clathrin- and caveolin-1-independent endocytosis: entry of simian virus 40 into cells devoid of caveolae. J. Cell Biol. **168:**477–488.
20. **Doherty, G. J., and H. T. McMahon.** 2009. Mechanisms of endocytosis. Annu. Rev. Biochem. **78:**857–902.
21. **Doxsey, S. J., F. M. Brodsky, G. S. Blank, and A. Helenius.** 1987. Inhibition of endocytosis by anti-clathrin antibodies. Cell **50:**453–463.
22. **Esfandiarei, M., and B. M. McManus.** 2008. Molecular biology and pathogenesis of viral myocarditis. Annu. Rev. Pathol. **3:**127–155.
23. **Hsu, K. H., K. Lonberg-Holm, B. Alstein, and R. L. Crowell.** 1988. A monoclonal antibody specific for the cellular receptor for the group B coxsackieviruses. J. Virol. **62:**1647–1652.
24. **Ilangumaran, S., A. Briol, and D. C. Hoessli.** 1998. CD44 selectively associates with active Src family protein tyrosine kinases Lck and Fyn in glycosphingolipid-rich plasma membrane domains of human peripheral blood lymphocytes. Blood **91:**3901–3908.
25. **Irie, T., E. Carnero, A. Okumura, A. Garcia-Sastre, and R. N. Harty.** 2007. Modifications of the PSAP region of the matrix protein lead to attenuation of vesicular stomatitis virus in vitro and in vivo. J. Gen. Virol. **88:**2559–2567.
26. **Ivanov, A. I.** 2008. Pharmacological inhibition of endocytic pathways: is it specific enough to be useful? Methods Mol. Biol. **440:**15–33.
27. **Ivanovic, T., M. A. Agosto, K. Chandran, and M. L. Nibert.** 2007. A role for molecular chaperone Hsc70 in reovirus outer capsid disassembly. J. Biol. Chem. **282:**12210–12219.
28. **Kirchhausen, T., E. Macia, and H. E. Pelish.** 2008. Use of dynasore, the small molecule inhibitor of dynamin, in the regulation of endocytosis. Methods Enzymol. **438:**77–93.
29. **Krishnan, M. N., B. Sukumaran, U. Pal, H. Agaisse, J. L. Murray, T. W. Hodge, and E. Fikrig.** 2007. Rab 5 is required for the cellular entry of dengue and West Nile viruses. J. Virol. **81:**4881–4885.
30. **Lamaze, C., A. Dujeancourt, T. Baba, C. G. Lo, A. Benmerah, and A. Dautry-Varsat.** 2001. Interleukin 2 receptors and detergent-resistant membrane domains define a clathrin-independent endocytic pathway. Mol. Cell **7:**661–671.
31. **Llorente, A., A. Rapak, S. L. Schmid, B. van Deurs, and K. Sandvig.** 1998. Expression of mutant dynamin inhibits toxicity and transport of endocytosed ricin to the Golgi apparatus. J. Cell Biol. **140:**553–563.
32. **Macia, E., M. Ehrlich, R. Massol, E. Boucrot, C. Brunner, and T. Kirchhausen.** 2006. Dynasore, a cell-permeable inhibitor of dynamin. Dev. Cell **10:**839–850.
33. **Marchant, D., A. Sall, X. Si, T. Abraham, W. Wu, Z. Luo, T. Petersen, R. G. Hegele, and B. M. McManus.** 2009. ERK MAP kinase-activated Arf6 trafficking directs coxsackievirus type B3 into an unproductive compartment during virus host-cell entry. J. Gen. Virol. **90:**854–862.
34. **Marsh, M., and A. Helenius.** 2006. Virus entry: open sesame. Cell **124:**729–740.
35. **Martino, T. A., M. Petric, H. Weingartl, J. M. Bergelson, M. A. Opavsky, C. D. Richardson, J. F. Modlin, R. W. Finberg, K. C. Kain, N. Willis, C. J. Gauntt, and P. P. Liu.** 2000. The coxsackie-adenovirus receptor (CAR) is used by reference strains and clinical isolates representing all six serotypes of coxsackievirus group B and by swine vesicular disease virus. Virology **271:** 99–108.
36. **Massol, R. H., J. E. Larsen, Y. Fujinaga, W. I. Lencer, and T. Kirchhausen.** 2004. Cholera toxin toxicity does not require functional Arf6- and dynamin-dependent endocytic pathways. Mol. Biol. Cell **15:**3631–3641.
37. **Mayer, M. P., and B. Bukau.** 2005. Hsp70 chaperones: cellular functions and molecular mechanism. Cell Mol. Life Sci. **62:**670–684.
38. **McNiven, M. A., H. Cao, K. R. Pitts, and Y. Yoon.** 2000. The dynamin family of mechanoenzymes: pinching in new places. Trends Biochem. Sci. **25:**115–120.
39. **Milstone, A. M., J. Petrella, M. D. Sanchez, M. Mahmud, J. C. Whitbeck, and J. M. Bergelson.** 2005. Interaction with coxsackievirus and adenovirus receptor, but not with decay-accelerating factor (DAF), induces A-particle formation in a DAF-binding coxsackievirus B3 isolate. J. Virol. **79:**655–660.
40. **Motley, A., N. A. Bright, M. N. Seaman, and M. S. Robinson.** 2003. Clathrin-mediated endocytosis in AP-2-depleted cells. J. Cell Biol. **162:**909–918.
41. **Nicoziani, P., F. Vilhardt, A. Llorente, L. Hilout, P. J. Courtoy, K. Sandvig, and B. van Deurs.** 2000. Role for dynamin in late endosome dynamics and trafficking of the cation-independent mannose 6-phosphate receptor. Mol. Biol. Cell **11:**481–495.
42. **Oh, P., D. P. McIntosh, and J. E. Schnitzer.** 1998. Dynamin at the neck of caveolae mediates their budding to form transport vesicles by GTP-driven fission from the plasma membrane of endothelium. J. Cell Biol. **141:**101–114.
43. **Orlandi, P. A., and P. H. Fishman.** 1998. Filipin-dependent inhibition of cholera toxin: evidence for toxin internalization and activation through caveolae-like domains. J. Cell Biol. **141:**905–915.
44. **Palade, G. E.** 1953. An electron microscope study of the mitochondrial structure. J. Histochem. Cytochem. **1:**188–211.
45. **Pang, H., P. U. Le, and I. R. Nabi.** 2004. Ganglioside GM1 levels are a determinant of the extent of caveolae/raft-dependent endocytosis of cholera toxin to the Golgi apparatus. J. Cell Sci. **117:**1421–1430.
46. **Parolini, I., M. Sargiacomo, F. Galbiati, G. Rizzo, F. Grignani, J. A. Engelman, T. Okamoto, T. Ikezu, P. E. Scherer, R. Mora, E. Rodriguez-Boulan, C. Peschle, and M. P. Lisanti.** 1999. Expression of caveolin-1 is required for the transport of caveolin-2 to the plasma membrane. Retention of caveolin-2 at the level of the golgi complex. J. Biol. Chem. **274:**25718–25725.
47. **Pelkmans, L., J. Kartenbeck, and A. Helenius.** 2001. Caveolar endocytosis of simian virus 40 reveals a new two-step vesicular-transport pathway to the ER. Nat. Cell Biol. **3:**473–483.
48. **Pelkmans, L., D. Puntener, and A. Helenius.** 2002. Local actin polymerization and dynamin recruitment in SV40-induced internalization of caveolae. Science **296:**535–539.
49. **Reagan, K. J., B. Goldberg, and R. L. Crowell.** 1984. Altered receptor specificity of coxsackievirus B3 after growth in rhabdomyosarcoma cells. J. Virol. **49:**635–640.
50. **Romero, J. R.** 2008. Pediatric group B coxsackievirus infections. Curr. Top. Microbiol. Immunol. **323:**223–239.
51. **Rothberg, K. G., J. E. Heuser, W. C. Donzell, Y. S. Ying, J. R. Glenney, and R. G. Anderson.** 1992. Caveolin, a protein component of caveolae membrane coats. Cell **68:**673–682.
52. **Sanchez-San Martin, C., T. Lopez, C. F. Arias, and S. Lopez.** 2004. Characterization of rotavirus cell entry. J. Virol. **78:**2310–2318.
53. **Saphire, A. C., T. Guan, E. C. Schirmer, G. R. Nemerow, and L. Gerace.** 2000. Nuclear import of adenovirus DNA in vitro involves the nuclear protein import pathway and hsc70. J. Biol. Chem. **275:**4298–4304.
54. **Scherer, P. E., R. Y. Lewis, D. Volonte, J. A. Engelman, F. Galbiati, J. Couet, D. S. Kohtz, E. van Donselaar, P. Peters, and M. P. Lisanti.** 1997. Cell-type and tissue-specific expression of caveolin-2. Caveolins 1 and 2 co-localize and

form a stable hetero-oligomeric complex in vivo. J. Biol. Chem. **272:**29337–29346.
55. **Shafren, D. R., R. C. Bates, M. V. Agrez, R. L. Herd, G. F. Burns, and R. D. Barry.** 1995. Coxsackieviruses B1, B3, and B5 use decay accelerating factor as a receptor for cell attachment. J. Virol. **69:**3873–3877.
56. **Shieh, J. T., and J. M. Bergelson.** 2002. Interaction with decay-accelerating factor facilitates coxsackievirus B infection of polarized epithelial cells. J. Virol. **76:**9474–9480.
57. **Singh, R. D., V. Puri, J. T. Valiyaveettil, D. L. Marks, R. Bittman, and R. E. Pagano.** 2003. Selective caveolin-1-dependent endocytosis of glycosphingolipids. Mol. Biol. Cell **14:**3254–3265.
58. **Smith, J. L., S. K. Campos, and M. A. Ozbun.** 2007. Human papillomavirus type 31 uses a caveolin 1- and dynamin 2-mediated entry pathway for infection of human keratinocytes. J. Virol. **81:**9922–9931.
59. **Spoden, G., K. Freitag, M. Husmann, K. Boller, M. Sapp, C. Lambert, and L. Florin.** 2008. Clathrin- and caveolin-independent entry of human papillomavirus type 16—involvement of tetraspanin-enriched microdomains (TEMs). PLoS ONE **3:**e3313.
60. **Stuart, A. D., H. E. Eustace, T. A. McKee, and T. D. Brown.** 2002. A novel cell entry pathway for a DAF-using human enterovirus is dependent on lipid rafts. J. Virol. **76:**9307–9322.
61. **Sturzenbecker, L. J., M. Nibert, D. Furlong, and B. N. Fields.** 1987. Intracellular digestion of reovirus particles requires a low pH and is an essential step in the viral infectious cycle. J. Virol. **61:**2351–2361.
62. **Sun, X., V. K. Yau, B. J. Briggs, and G. R. Whittaker.** 2005. Role of clathrin-mediated endocytosis during vesicular stomatitis virus entry into host cells. Virology **338:**53–60.
63. **Superti, F., L. Seganti, F. M. Ruggeri, A. Tinari, G. Donelli, and N. Orsi.** 1987. Entry pathway of vesicular stomatitis virus into different host cells. J. Gen. Virol. **68:**387–399.
64. **Torgersen, M. L., G. Skretting, B. van Deurs, and K. Sandvig.** 2001. Internalization of cholera toxin by different endocytic mechanisms. J. Cell Sci. **114:**3737–3747.
65. **Traub, L. M.** 2003. Sorting it out: AP-2 and alternate clathrin adaptors in endocytic cargo selection. J. Cell Biol. **163:**203–208.
66. **Tsai, B., J. M. Gilbert, T. Stehle, W. Lencer, T. L. Benjamin, and T. A. Rapoport.** 2003. Gangliosides are receptors for murine polyoma virus and SV40. EMBO J. **22:**4346–4355.
67. **van der Bliek, A. M., T. E. Redelmeier, H. Damke, E. J. Tisdale, E. M. Meyerowitz, and S. L. Schmid.** 1993. Mutations in human dynamin block an intermediate stage in coated vesicle formation. J. Cell Biol. **122:**553–563.
68. **Van Hamme, E., H. L. Dewerchin, E. Cornelissen, B. Verhasselt, and H. J. Nauwynck.** 2008. Clathrin- and caveolae-independent entry of feline infectious peritonitis virus in monocytes depends on dynamin. J. Gen. Virol. **89:**2147–2156.
69. **Wang, X., and J. M. Bergelson.** 1999. Coxsackievirus and adenovirus receptor cytoplasmic and transmembrane domains are not essential for coxsackievirus and adenovirus infection. J. Virol. **73:**2559–2562.
70. **Whitbeck, J. C., C. H. Foo, M. Ponce de Leon, R. J. Eisenberg, and G. H. Cohen.** 2009. Vaccinia virus exhibits cell-type-dependent entry characteristics. Virology **385:**383–391.
71. **Yousef, G. E., I. N. Brown, and J. F. Mowbray.** 1987. Derivation and biochemical characterization of an enterovirus group-specific monoclonal antibody. Intervirology **28:**163–170.
72. **Yousef, G. E., G. F. Mann, I. N. Brown, and J. F. Mowbray.** 1987. Clinical and research application of an enterovirus group-reactive monoclonal antibody. Intervirology **28:**199–205.
73. **Zaremba, S., and J. H. Keen.** 1983. Assembly polypeptides from coated vesicles mediate reassembly of unique clathrin coats. J. Cell Biol. **97:**1339–1347.